Journal of Radioanalytical and Nuclear Chemistry (2022) 331:129–144
https://doi.org/10.1007/s10967-021-08094-z

Trace and major elements, natural and artificial radionuclides assessment in bottom sediments from Tietê River basin, São Paulo State, Brazil: part III

Barbara P. Mazzilli[1] · Letícia G. S. Lavieri[1] · Josiane S. Soares[2] · Flavio R. Rocha[2] · Matheus Angelini[2] · Deborah I. T. Favaro[2]

Received: 29 June 2021 / Accepted: 30 October 2021 / Published online: 21 November 2021

Abstract
This paper aims at quantifying natural and artificial radionuclides, trace and major elements in sediments collected along the Tietê River basin. The results obtained for Cd, Cr, Cu, Ni and Zn, indicated that the region of "High Tietê" is highly polluted, followed by the region of "Middle Tietê" and the region of "Low Tietê" does not present evidence of contamination. The natural radionuclide concentrations were of the same order of magnitude of world average values and can be defined as basal levels of the region. Cesium-137 activity concentration ranged from 0.22 ± 0.08 Bq kg^{-1} to 0.96 ± 0.12 Bq kg^{-1}.

Keywords Heavy metals · Major and trace elements · Radionuclides · River sediments

Introduction

The Tietê River with 1100 km of extension is the most important river in the State of São Paulo. Its drainage basin, with a population of more than 25 million people, is important for food and energy production, with more than ten hydroelectric power plants along the main channel of the river and tributaries [1]. Some of these dams operate with a lock system allowing river navigation, facilitating the transport of the region products, at a lower cost than road transport. The Tietê River is navigable for more than 450 km in its watercourse. Associated with this important system, which has a great impact on the river's natural conditions, there is also the intense loss of riparian forest due to urban and rural expansion, as well as the release of pollutants from cities located on its banks and their tributaries. The main causes of the degradation of the quality of water are point sources of pollution (sewage and industrial effluents) and diffuse (urban and agricultural drainage), in addition to atmospheric precipitation. In evaluating the impact caused by human activities on the contamination of aquatic environments, the assessment of sediment quality is essential for diagnosing current conditions and taking future measures. Due to the severe impact and degradation of the Tietê River, a project entitled ''Evaluation of pollution by metals and trace elements in river sediments—case study of Tietê River, State of São Paulo, Brazil'' was proposed. The aim of this project was to determine the mass fraction and distribution of major and some trace elements potentially contaminants in bottom sediments along the Tietê River basin.

Due to the great extent of the collecting area, it has already been suggested by Campos [2] the division of the river into three regions, taking into account the occupation of the soil and the use of water resources of each region. Campos named "High Tietê Region"—HTR the upper part of the river, which corresponds to the sampling points T1A to T3C. This region is highly populated and industrialized. The medium part of the river was named "Middle Tietê Region"—MTR, with sampling points T4 to T23. In this part the river crosses the region of Campinas, where a great industrial and agricultural expansion occurred in the last years. In this region the river receives input from important tributaries such as Sorocaba, Jundiaí, Capivari

✉ Barbara P. Mazzilli
mazzilli@ipen.br

[1] Laboratório de Radiometria Ambiental (LRA-CEMRI), Instituto de Pesquisas Energéticas e Nucleares, (IPEN – CNEN/SP), Av. Prof. Lineu Prestes 2242, São Paulo 05508-000, Brazil

[2] Laboratório de Análise Por Ativação com Nêutrons (LAN-CERPQ), Instituto de Pesquisas Energéticas e Nucleares, (IPEN – CNEN/SP), Av. Prof. Lineu Prestes 2242, São Paulo 05508-000, Brazil

and Piracicaba rivers. In the last part, the name "Low Tietê Region"—LTR was adopted, comprising the sampling points T24 to T34; this region occupation is mainly agricultural.

In the first phase of this study, Rocha et al. [3] analyzed major and trace elements in 12 sediment samples collected along the HTR. They observed a high variation in the element's concentration, strongly dependent on the occupation of the region. The higher impact was found in the metropolitan region of São Paulo, where contamination was observed for As, Cr and Zn.

In the second phase of this study, Favaro et al. [4] analyzed major and trace elements in 15 sediment samples, collected in the Middle Tietê Region—MTR. The authors concluded that the metals As and Zn presented high values for the enrichment factor and geoaccumulation index, indicating anthropogenic inputs.

As a complementary study, the present paper aims at quantifying natural (^{238}U, ^{226}Ra, ^{210}Pb, ^{232}Th, ^{228}Ra and ^{40}K) and artificial (^{137}Cs) radionuclides in sediments along the whole river; major and trace elements (As, Cd, Co, Cr, Cu, Ni, Pb and Zn) in sediments collected along the LTR, in order to evaluate the basal level of these elements and the extent of contamination.

Materials and methods

Sediment sampling and sample measurement

Forty bottom sediment samples were collected along the Tietê River from 2012 to 2014, in 6 sampling campaigns. The sampling locations were chosen taking into account the contribution of the drainage basins responsible for bringing the polluting load to the river (Fig. 1). Detail of the sediment sampling and sample preparation have already been described in previous studies [3, 4].

The macro and trace elements of interest were analyzed using the appropriate methodologies for each element determination. For major element determination in sediments, the X-ray fluorescence spectrometry (XRF) analytical technique was used. The elements Cu and Ni were determined by inductively coupled plasma-optical emission spectrometry (ICP-OES); the elements Cd and Pb were determined by graphite-furnace atomic absorption spectrometry (GF-AAS); the mass fraction of As, Co, Cr, U, Th and Zn was determined by using instrumental neutron activation analysis (INAA); the activity concentration of radionuclides, ^{226}Ra, ^{228}Ra, ^{210}Pb, ^{40}K and ^{137}Cs, was determined by high resolution gamma ray spectrometry. The granulometric composition of the sediments along the whole river was determined by the pipetting method and Organic Matter (OM) content was determined by the photometric method.

Determination of As, Co, Cr, Th, U and Zn by instrumental neutron activation analysis (INAA)

Approximately 150 mg of sediment (in duplicate) and standard reference materials were weighed in pre-cleaned double polyethylene bags for irradiation. Sediment samples and reference materials were irradiated for approximately 7 h, under a thermal neutron flux of $1–5 \times 10^{12}$ n cm^{-2} s^{-1} at the IEA-R1 nuclear research reactor at IPEN. The following elements were determined: As, Co, Cr, Th, U and Zn. Detail of the analytical methodology are described in Larizzatti et al. [5]. The combined uncertainty [*uc*] was evaluated following ISO GUM procedure. The combined uncertainty (*uc*) was evaluated by taking into account the counting statistics (*ustat*) (major contribution), certified reference material uncertainties (*uCRM*) and sample and reference materials masses (*umass*), using a coverage factor $k = 2$. Relative expanded uncertainties (U, %) were less than the corresponding relative variation coefficients (CV, %), confirming the suitability of the method for the analysis of these elements. Methodology validation was performed by analyzing the reference materials BE-N (Basalt-IWG-GIT) from Centre de Recherches Pétrographiques et Géochimiques, France, Soil-5 (IAEA-S-5) and Lake Sediment (IAEA-SL-1). Results of relative standard deviation ranged from 2.2 to 9.2%, relative errors from 1.0 to 10.8%, confirming adequate precision and accuracy. The Z-score values found were /Z-score/ < 2, confirming the adequacy of the INAA analytical technique, according to Konieczka & Namiesnik (2009) [6].

Determination of Cu and Ni by inductively coupled plasma-optical emission spectrometry (ICP-OES) and Cd and Pb by graphite-furnace atomic absorption spectrometry (GF-AAS)

The digestion of samples and reference materials was performed using the CEM microwave program, model MARS-6, according to USEPA method 3051A [7]. About 500 mg of sediment sample and 250 mg of each reference material were weighed directly into the TEFLON® tubes and 10 mL of the mixture (7.5 HNO3:2.5 HCl conc) (3:1) was added for the sample digestion. After digestion and cooling of the tubes, samples, reference materials and blank were filtered, and the volume made up to 50 mL with Milli-Q ultrapure water. Thus, the samples were ready for reading in the ICP-OES equipment for the elements Cu and Ni and in the GF-AAS, for the metals

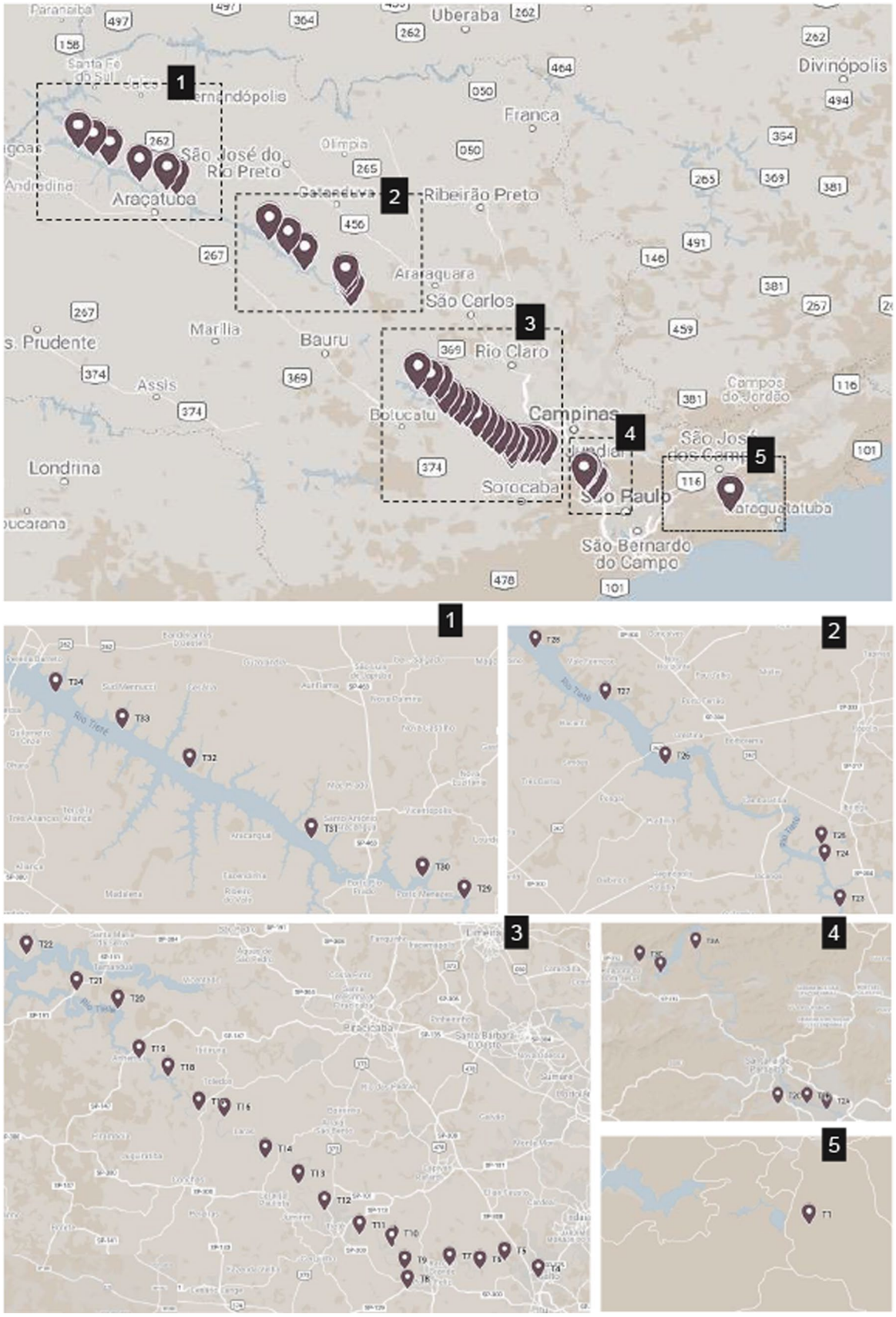

Fig. 1 Sediment sampling location along the Tietê River Basin

Cd and Pb. The samples were quantified in the ICP-OES MPX-Varian equipment of the Chemical Analysis Laboratory –LAQ /IPT-SP and in the AANALYST 800 of Perkin Elmer, of the Atomic Absorption Laboratory of LAN-IPEN. The validation of the analytical methodologies, in terms of precision and accuracy, was carried out through the analysis of the reference material EnviroMAT SS-2 (Soil Contaminated from SCP Science Laboratory) and Sandy Clay1 (CRM049-trace metal) from Merck-Sigma Aldrich, which have certified values of total concentration for all elements of interest and concentration ranges for the USEPA 3051A digestion procedure [7]. The analytical methodology validation procedure followed the INMETRO guide [8] and the results were expressed in terms of trend/recovery in % and in expanded uncertainty for each element. The expanded uncertainties for both analytical techniques were calculated by using a coverage factor ($k = 2$) and the combined uncertainties, considering the uncertainty contribution of the mass fraction values, calibration curve, analytical blank, volume, dilution factor and mass. Details of the uncertainty calculation by the GF-AAS analytical technique are described in Tappiz & Moreira [9]. As in the INAA technique, the relative expanded uncertainties (U, %) were smaller than the corresponding relative variation coefficients (CV, %), confirming the suitability of the methods for metal analyses. For the Sandy Clay certified reference material analyses, the relative standard deviations (RSD) were 2.4% for Cd and 1.6% for Ni; relative errors (RE) were 6.8% and 8.2% respectively for Cd and Ni. For the SS-2 certified reference material analyses, RSDs were 1.9% for Cd and 3.5% for Pb, and RE 8.7% for Pb. There was no certified concentration value for Cd in this CRM. In the ICP-OES analytical technique, the Sandy Clay RSDs were 9.4% (Cu) and 9.9% (Ni), and the REs were 5.2% and 2.1% respectively. For the SS-2 certified reference material analyses the RSDs were 2.9% (Cu) and 10.4% (Ni), and the REs were 9.9% (Cu) and 11.1% (Ni). Some measurements presented analytical biases that could affect the results. However, the potential biases would be a relatively small contribution to the data variation compared to natural and anthropometric effects found in this study.

Determination of major elements by XRF

The X-ray fluorescence spectrometry (XRF) analytical technique was used for major element determination in sediments. Samples were prepared according to Mori et al. [10] at the XRF Laboratory—NAP Geoanalítica—USP, Institute of Geosciences, University of São Paulo, and the measurements were carried out in an X-Ray Philips PW 2400 spectrometer. The precision and accuracy of the analytical methodology were evaluated by measuring the JB-1[a] and JG 1[a] reference materials (Geological Survey of Japan) [11]. The precision of these measurements, given by the relative standard deviation (RSD), was better than 5%, and the relative errors (accuracy) ranged from 0.2 to 4.2% in the JB1[a] certified reference material and from 0.4 to 10.1% for the JG1[a] certified reference material. Some measurements presented analytical biases that could affect the results. However, the potential biases would be a relatively small contribution to the data variation compared to natural and anthropometric effects found in this study. Major elements were determined by wavelength-dispersive XRF using fused glass discs. The major elements determined were SiO_2, TiO_2, Al_2O_3, Fe_2O_3, MnO, MgO, CaO, Na_2O and P_2O_5. The results for samples T1A to T22 were determined in previous studies [3, 4]. The results for sediment samples T23 to T34 were determined in this paper.

Determination of ^{226}Ra, ^{228}Ra, ^{210}Pb, ^{40}K and ^{137}Cs by gamma spectrometry

The sediment samples were dried until constant weight and sieved at 60 mesh. Samples weighing 100 g were sealed in polyethylene containers for 30 days to allow the radioactive equilibrium between ^{226}Ra and its decay products gamma emitters. The activity measurement of ^{226}Ra, ^{228}Ra and ^{210}Pb, ^{40}K and ^{137}Cs was undertaken by gamma spectrometry, with a Hyper Pure Germanium detector HPGe, GX2518 with 25% relative efficiency, from CAMBERRA, during 86,000 s. The radionuclide ^{226}Ra was determined taking into account the mean value of the photo peaks of the radionuclides: ^{214}Pb (295.21 keV and 351.92 keV) and ^{214}Bi (609.31 keV and 1120.30 keV). The radionuclide ^{228}Ra was determined by measuring the intensity of the photo peaks 911.07 keV and 969.11 keV from ^{228}Ac. The radionuclide ^{210}Pb was measured through its photo peak of 46.50 keV, after correction of the auto absorption of the low energy gamma rays by the sample, according to Cutshall et al. [12]. The ^{40}K was measured through its photo peak of 1460 keV and ^{137}Cs through the photo peak of 661.66 keV. Multichannel Maestro A65-I model software was used for the spectrum acquisition and determination of the net peak area; the WinnerGamma/Interwinner 6.01 software from Eurisys Measures was used for the analysis of gamma-ray spectra, evaluation of concentrations and associated uncertainties. Background spectra were obtained by measuring ultrapure water in the same counting geometry used for the samples. The counting efficiency curve was obtained by using standard reference solutions from Amersham. The performance of the laboratory to measure radionuclides by gamma spectrometry was carried out by participating in independent Proficiency Tests organized by International Atomic Energy

Agency—IAEA and by Instituto de Radioproteção e Dosimetria (IRD) in Brazil.

Silt, clay and sand content, Organic Matter (OM) determination

These determinations were carried out at the Instituto Agronômico de Campinas (IAC). The granulometric analyses (pipetting method) and OM (photometric method) were carried out according to Camargo et al. [13].

Results and discussion

Grain size and major element distribution of the sediments

The sediments come from the physicochemical processes of weathering of rocks and soils; therefore, it is important to highlight the characterization of the region's lithology. The region near the source of the Tietê River is formed basically by granites and migmatites and the soils are of the reddish yellow podzolic type. In the Middle Tietê sandstones are predominant, while the soil is of the reddish-yellow and dark red latosol type, and finally the Low Tietê is characterized by a lithological uniformity mainly formed by sandstones and the soils are of the dark red latosol type [14].

The grain size distribution of the sediments, the OM content and the major element content are presented in Table 1. The granulometric composition of most sediment samples collected along the Tietê River presented a high sand content (> 50%), as we can observe in the clay-silt-sand ternary discriminating diagram (Fig. 2, left). A discriminating ternary diagram Al_2O_3–MgO + CaO – Na_2O + K_2O (Fig. 2, right) shows that most samples plot near the Al_2O_3 component, reflecting the presence of kaolinite in the clay fraction. Along the riverbed there is a great lithological variety, including mainly gneissic, basaltic and sandstone rocks. The sediments derived from them are mature, composed essentially of quartz and secondly of kaolinite and sericite, being, therefore, chemically rich in SiO_2 and Al_2O_3 and poor in alkaline and alkaline-earth elements.

Metal's mass fraction in the sediments

The element´s mass fraction in the sediment samples and the North American Shale Composite (NASC) values [15] are presented in Fig. 3. The concentration obtained in this study for the majority of the elements presented significant variations in relation to the global geological reference values and presented also differences between the concentrations of the same element in different regions of the basin, due to the lithological variations of each region and textural composition of the sediment samples. The upper Tietê basin (HTR, points T1A to T3C) is densely inhabited and has the highest concentration of industries along the length of the river, receiving continuous discharges of effluents from this population, in addition to changes in its bed over the years [3]. The points located in Salesópolis (T1A to T1C) present the lowest concentrations, due to their proximity to the source of the river and the fact that in the region there are no large concentrations of population and effluent discharge into the river. Points T2 (T2A, 2B, 2C) and T3 (T3A, 3B, 3C) are located right after the river crosses the city of São Paulo, receiving a large part of the material from the inadequate disposal of untreated sewage and the contribution of pollution from tributaries such as the Pinheiros River, for example. It is possible to observe, in the Middle Tietê region (points from T4 to T23), that there is still a great variation in the concentration of the elements studied, indicating that there are still factors impacting the region. This stretch is characterized not only by population occupation, but also by the strong influence of industrial and agricultural occupation. In addition, this region receives important tributaries, Jundiai, Capivari, Piracicaba and Sorocaba rivers that contribute to the increase of the sediment deposition. Finally, the Low Tietê region, points T24 to T34, predominantly focused on agriculture, presented the lowest concentration values, below the NASC values, for all elements studied.

The box plot of the elements analyzed divided per region is depicted in Fig. 4. In the HTR region, all the elements analyzed, except for Co, presented a larger distance between the first and third quartiles, which implies a great dispersion in the mass fraction. This should be indeed expected because HTR is the most industrialized and populated region, and, hence, with the largest source of input contamination. In the MTR region, there was a marked decrease between the first and the third quartiles, indicating a lower dispersion of the results along this stretch of the river. A greater dispersion was observed only for As. In the LTR region, a different behavior was observed: larger distances between the first and the third quartiles for As and Co; a smaller distance for Cr and Cu and almost no variation in mass fraction for Cd, Ni, Pb and Zn. Considering the median of the mass fraction, the elements As, Cd, Cu, Ni, Pb and Zn presented a decreasing from HTR to MTR and to LTR. Yet, for Cr and Co, the order was HTR > LTR > MTR. Except for Co and Cr, LTR values were the lowest mass fraction for all elements and presented the smaller variability. Therefore, these values may be associated to the natural occurrence of these elements, in contrast with the MTR and specially HTR sediment groups, in which anthropogenic impacts are more pronounced.

It is also observed that:

Table 1 Grain size distribution, OM and major element contents (%) of sediments from Tietê River according to the regions: HTR, MTR and LTR

	Clay %	Silt %	Sand %	Fines %	OM (g/cm^3)	SiO_2	TiO_2	Al_2O_3	Fe_2O_3	MnO	MgO	CaO	Na_2O	K_2O	P_2O_5	Total	SiO_2/Al_2O	Fe_2O_3/SiO_2	$MnO/SiO_2 \times 10^4$	Tietê Region
T1A	8.70	4.80	86.5	13.5	–	83.32	0.491	7.66	1.08	0.026	0.22	0.11	0.28	2.84	0.054	99.8	10.9	0.013	3.1	HTR
T1B	18.7	5.90	75.4	24.6	29	82.10	0.345	8.34	1.21	0.020	0.15	0.10	0.23	2.21	0.058	100.3	9.8	0.015	2.4	
T1C	68.1	28.4	3.50	96.5	–	41.11	0.891	27.71	4.13	0.035	0.32	0.09	0.08	0.79	0.252	100.4	1.5	0.100	8.5	
T2A	5.70	10.4	83.9	16.1	9	61.60	0.973	16.32	5.91	0.051	0.69	0.78	0.40	1.71	0.496	99.8	3.8	0.096	8.3	
T2B	27.7	49.6	22.7	77.3	–	59.57	0.929	17.29	5.39	0.046	0.67	0.97	0.40	1.93	0.527	99.6	3.4	0.090	7.7	
T2C	32.0	34.9	33.1	66.9	–	59.31	0.925	17.34	5.39	0.047	0.67	0.96	0.41	1.91	0.522	99.7	3.4	0.091	7.9	
T3A	22.0	28.0	50.0	50.0	26	55.86	0.969	19.70	6.19	0.050	0.64	0.72	0.33	1.85	0.642	99.8	2.8	0.111	9.0	
T3B	14.5	23.2	62.3	37.7	–	67.44	0.950	15.10	4.50	0.049	0.70	0.79	0.44	1.99	0.325	99.9	4.5	0.067	7.3	
T3C	26.9	44.4	28.7	71.3	–	49.92	1.041	22.65	6.55	0.053	0.79	0.88	0.36	1.94	0.603	99.3	2.2	0.131	10.6	
T4	6.90	7.30	85.8	14.2	19	83.48	0.648	7.01	2.05	0.039	0.23	0.28	0.32	1.94	0.226	100.1	11.9	0.025	4.7	MTR
T5	16.5	19.1	64.4	35.6	21	80.56	0.490	7.43	2.51	0.040	0.26	0.32	0.22	1.14	0.397	99.8	10.8	0.031	5.0	
T6	14.9	15.4	69.7	30.3	20	79.77	0.688	8.75	2.81	0.059	0.27	0.27	0.25	1.59	0.357	99.9	9.1	0.035	7.4	
T7	10.0	10.2	79.8	20.2	15	83.26	0.557	7.44	2.23	0.043	0.23	0.23	0.28	1.57	0.289	99.8	11.2	0.027	5.2	
T8	12.2	10.8	77.0	23.0	18	82.35	0.547	7.06	2.36	0.052	0.12	0.26	0.02	1.41	0.394	98.7	11.7	0.030	6.3	
T9	11.0	14.3	74.7	25.3	–	79.85	0.580	8.35	2.82	0.062	0.19	0.31	0.09	1.63	0.483	98.8	9.6	0.040	7.8	
T10	5.90	5.00	89.1	10.9	–	87.01	0.505	5.39	1.79	0.039	0.08	0.20	0.05	1.45	0.262	99.1	16.1	0.020	4.5	
T11	17.3	17.9	64.8	35.2	–	74.24	0.668	10.91	3.57	0.062	0.23	0.28	0.07	1.62	0.617	99.0	6.8	0.050	8.4	
T12	20.4	26.7	52.9	47.1	25	74.69	0.682	10.40	3.60	0.074	0.23	0.32	0.07	1.50	0.604	98.6	7.2	0.050	9.9	
T13	34.5	49.1	16.4	83.6	37	54.61	0.936	19.83	6.69	0.113	0.46	0.50	0.05	1.71	1.102	98.7	2.8	0.120	20.7	
T14	13.7	16.0	70.3	29.7	26	79.45	0.764	8.63	3.11	0.052	0.19	0.22	0.03	1.29	0.247	99.7	9.2	0.040	6.5	
T15	18.0	21.5	60.5	39.5	24	76.79	0.677	9.61	3.62	0.086	0.21	0.33	0.09	1.52	0.715	99.6	8.0	0.050	11.2	
T16	19.0	25.2	55.8	44.2	27	75.91	0.670	9.45	3.53	0.084	0.20	0.32	0.08	1.49	0.702	98.5	8.0	0.050	11.1	
T17	27.9	45.2	26.9	73.1	37	61.86	0.822	15.45	5.64	0.120	0.41	0.45	0.08	1.58	1.182	98.6	4.0	0.090	19.4	
T18	41.3	52.8	5.90	94.1	40	52.34	1.018	20.58	7.18	0.108	0.56	0.52	0.02	1.56	0.972	98.6	2.5	0.140	20.6	
T19	15.4	15.7	68.9	31.1	17	81.82	0.560	7.28	2.56	0.047	0.26	0.23	0.22	1.25	0.307	98.5	11.2	0.030	5.7	
T20	36.4	49.4	14.2	85.8	36	58.60	0.942	17.68	5.99	0.090	0.65	0.50	0.19	1.55	0.826	99.0	3.3	0.100	15.4	
T21	0.40	4.50	95.1	4.90	2	96.09	0.117	1.50	0.27	0.004	0.05	0.04	< 0.02	0.56	0.021	99.6	64.1	0.00	0.4	
T22	24.8	7.50	67.7	32.3	13	77.18	0.575	8.27	3.62	0.138	0.27	0.16	< 0.02	0.36	0.359	98.5	9.3	0.05	17.9	
T23	28.6	28.2	43.2	56.8	40	32.69	4.619	16.13	20.90	0.343	0.82	4.13	0.28	0.74	0.547	98.6	2.0	0.64	104.9	
T24	27.7	25.0	47.3	52.7	28	35.42	7.225	15.08	26.79	0.296	0.70	0.69	0.04	0.41	0.395	98.9	2.3	0.76	83.6	LTR
T25	5.50	2.30	92.2	7.8	5	81.15	1.710	4.62	6.18	0.078	0.09	0.82	< 0.02	0.06	0.136	99.3	17.6	0.076	9.6	
T26	43.8	6.10	50.1	49.9	3	63.27	2.118	14.41	8.42	0.061	0.92	0.15	< 0.02	1.14	0.148	98.7	4.4	0.133	9.6	
T27	3.80	3.50	92.7	7.3	10	89.43	0.941	3.20	1.08	0.022	0.06	0.05	< 0.02	0.07	0.037	99.2	27.9	0.012	2.5	
T28	3.00	2.50	94.5	5.5	2	92.16	0.545	2.79	1.70	0.020	0.26	0.09	0.09	1.02	0.038	100.3	33.0	0.018	2.2	

Table 1 (continued)

	Clay %	Silt %	Sand %	Fines %	OM (g/cm^3)	SiO_2	TiO_2	Al_2O_3	Fe_2O_3	MnO	MgO	CaO	Na_2O	K_2O	P_2O_5	Total	SiO_2/Al_2O	Fe_2O_3/SiO_2	MnO/SiO_2 × 10^4	Tietê Region
T29	17.7	16.2	66.1	33.9	36	76.35	1.600	6.50	4.23	0.098	0.14	0.17	< 0.02	0.24	0.114	99.0	11.7	0.055	12.8	
T30	12.8	5.40	81.8	18.2	25	75.28	1.962	5.28	7.99	0.086	0.09	0.14	< 0.02	0.08	0.109	98.8	14.3	0.106	11.4	
T31	7.70	5.40	86.9	13.1	34	87.30	1.148	2.28	3.09	0.074	0.08	0.05	< 0.02	0.17	0.035	99.2	38.3	0.035	8.5	
T32	35.7	16.8	47.5	52.5	46	61.62	1.876	9.45	10.47	0.100	0.18	0.18	< 0.02	0.09	0.152	99.1	6.5	0.170	16.2	
T33	19.3	4.60	76.1	23.9	6	85.96	0.997	5.08	2.96	0.031	0.04	0.04	< 0.02	0.05	0.024	98.7	16.9	0.034	3.6	
T34	10.6	3.00	86.4	13.6	12	92.91	0.466	2.11	1.34	0.016	0.02	0.03	< 0.02	0.05	0.016	99.0	44.0	0.014	1.7	
Not determined																				

- As presented three outliers in the MTR (T13, T18 and T20);
- Cr presented one outlier (T13);
- Pb presented two outliers (T13 and T18);
- Zn and Ni presented one outlier in the LTR (T24).

The grain size of all these outlier points presented high levels of fine sediments (silt + clay), T13 (83.6%), T18 (94.1%), T20 (85.8%) and T24 (52.7%). These points also presented a higher OM content. This behavior can explain the higher mass fraction values found for metals and metalloid As and the outlier values in the MTR region since, in general, the concentrations obtained for the other sampling points were much lower than those in the HTR region.

A different pattern was observed for the box plot of Co, in which the LTR presented the higher variation in the sediment's mass fraction. This element presented upper outliers in three regions, which are associated with high content of sand, points T2A (HTR, 83.9% of sand); T23 (MTR, 43.2% of sand) and T24 (LTR, 47.3% of sand). Point T1A presented a lower outlier for Co (86.5% of sand). Co presented sediment mass fraction below the NASC value (28 mg kg^{-1}) along the Tietê River basin, except for T2A, T23 and T24 points (Fig. 3).

Similar studies for the Tietê River and other rivers in Brazil and worldwide were already published in Favaro et al. [4].

Contamination assessment by applying Threshold Effect Level (TEL) and Probable Effect Level (PEL) guiding values

In order to evaluate the quality of the sediments, their concentrations were compared with TEL (Threshold Effect Level) and PEL (Probable Effect Level) guiding values established by the Canadian Council of Ministers of the Environment-CCME [16].

In Fig. 3, the sediment's mass fraction distribution is presented with the TEL and PEL values. The elements As and Pb did not present values above PEL, almost all the As and Pb concentrations are below TEL values, except for HTR; in the two former locations the sediments are classified as "Very good" and "Good" for these elements. Silva et al. [17] reported background values for As ranging from 6.3 to 12 mg kg^{-1}, for Baixada Santista, on the coast of the State of São Paulo, depending on the grain size sediment fraction. These results indicate that As may be enriched in São Paulo soil, in values over the global average (2.0 mg kg^{-1}) and TEL value (5.9 mg kg^{-1}).

The metals Cr, Ni and Zn, exceeded the PEL values in the points T2 (2A, 2B, 2C) and T3 (3A, 3B, 3C), HTR, in these locations the quality of the sediments is classified as "very

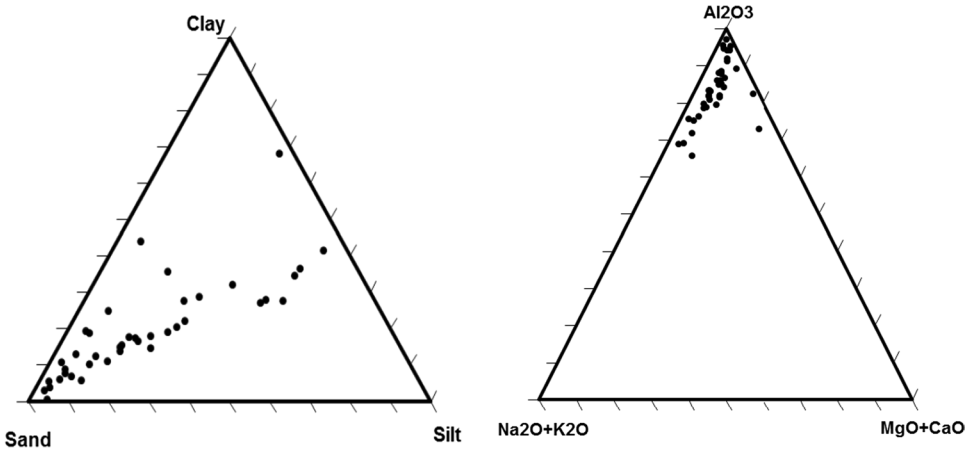

Fig. 2 Clay-Silt-Sand and Al_2O_3–MgO + CaO–$Na_2O + K_2O$ ternary discriminating diagrams for the sediment samples from T1A to T34

poor", being the worst situation for these metals. For Cd and Cu the sediments can be classified as of "regular quality" in the HTR and "good" and "very good" quality in the MTR and LTR, respectively.

The basal levels for the elements Cd, Cu, Ni and Zn can be considered as the concentrations found in the region of Low Tietê, which are close to the NASC values. The result of Cr reveals that the sediment pollution occurs along the entire length of the river, the use of agrochemicals being the main source of contamination. The anthropogenic input of Cu is mainly due to the use of $CuSO_4$, which is used to control algae production in hydroelectric reservoirs. The element Zn presented values that surpassed PEL values (315 mg kg^{-1}), for T2 (2A, 2B, 2C), T3 (3A, 3B, 3C), T5, T11, T12, T13, T16, T17, T18 and T20, with "bad" or "poor" sediment quality classification.

Taking into account that the values above PEL are an indication of impact in the region, it can be concluded that the High Tietê region is contaminated for Cd, Cr, Cu, Ni and Zn, followed by the Middle Tietê region, in a lower scale, confirming the need for mitigation measures in these regions.

Contamination assessment by applying the Geoaccumulation Index (*IGeo*)

The Geoaccumulation Index (*IGeo*) was used here as a second criterion to assess the contamination of sediments [18, 19], by using the following equation:

$$IGeo = log_2\left(\frac{C_{sam}}{1.5C_{ref}}\right)$$

where, C_{sam} is the concentration of the element in the sediment sample and C_{ref} is the concentration of the element in the reference material. The classification of the contamination levels from *IGeo* values is: 0 (basal level); from 0 to 1 (unpolluted to moderately polluted); from 1 to 2 (moderately polluted); from 2 to 3 (moderately to strongly polluted); from 3 to 4 (strongly polluted); from 4 to 5 (strongly to extremely polluted) and > 5 (extremely polluted).

In this study, it was used instead of the NASC reference values for C_{ref}, those from Nascimento et al. [20], referred to as C_1, which represents the status of the river in 2008 for HTR, MTR and LTR, and C_2 for C_{sam} in the current situation, so that

$$IGeo = log_2\left(\frac{C_2}{1.5C_1}\right) = log_2\left(\frac{C_2}{C_1}\right) - log_2 1.5 = log_2\left(\frac{C_2}{C_1}\right) - 0.58$$

Notice that the difference between the current status and the situation in 2008 is given by

$$\Delta = log_2\left(\frac{C_2}{C_1}\right) = IGeo + 0.58$$

so that, an *IGeo* value of −0.58 would indicate no change; any value larger than −0.58 would mean that the situation has gotten worse; and values less than −0.58 would mean that it has gotten better.

The results of *IGeo* for the elements As, Cd, Cr, Cu, Ni, Pb and Zn, in the bottom sediment in the region HTR, MTR and LTR, are presented in Fig. 5. According to the results obtained, the only elements that presented *IGeo* > -0.58, indicating an increase in the degree of pollution, are Cd, Cr, Cu, Ni and Zn, mainly in the sediments from HTR. The elements Cd and Zn presented values $2 < IGeo < 3$, classifying these sediments as "moderately to strongly polluted" and only one point for Cd presented $IGeo > 3$, classifying this point as "strongly polluted" (HTR).

The elements As and Pb presented $IGeo < -0.58$ along the river basin, indicating a decrease in the contamination, and consequently evidence that there was an improvement in the quality of the sediments, in relation to these elements, over the last 12 years. Anyway, it is important to emphasize

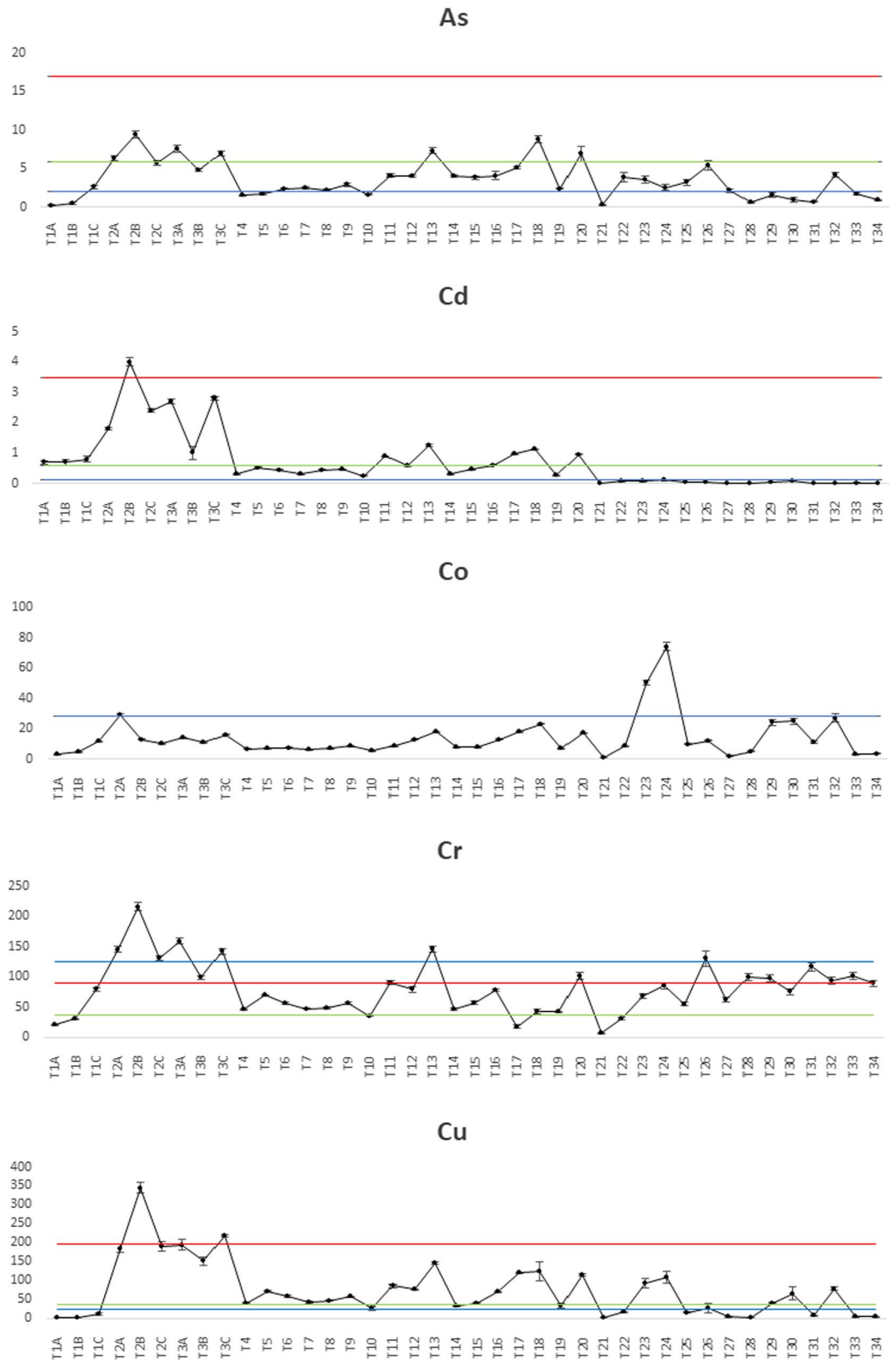

Fig. 3 Sediment's mass fraction distribution (mg kg^{-1}) along the Tietê River, NASC values (blue line), Probable Effect Level-PEL (red line) and Threshold Effect Level-TEL (green line). Error bars represent expanded uncertainties at $k = 2$

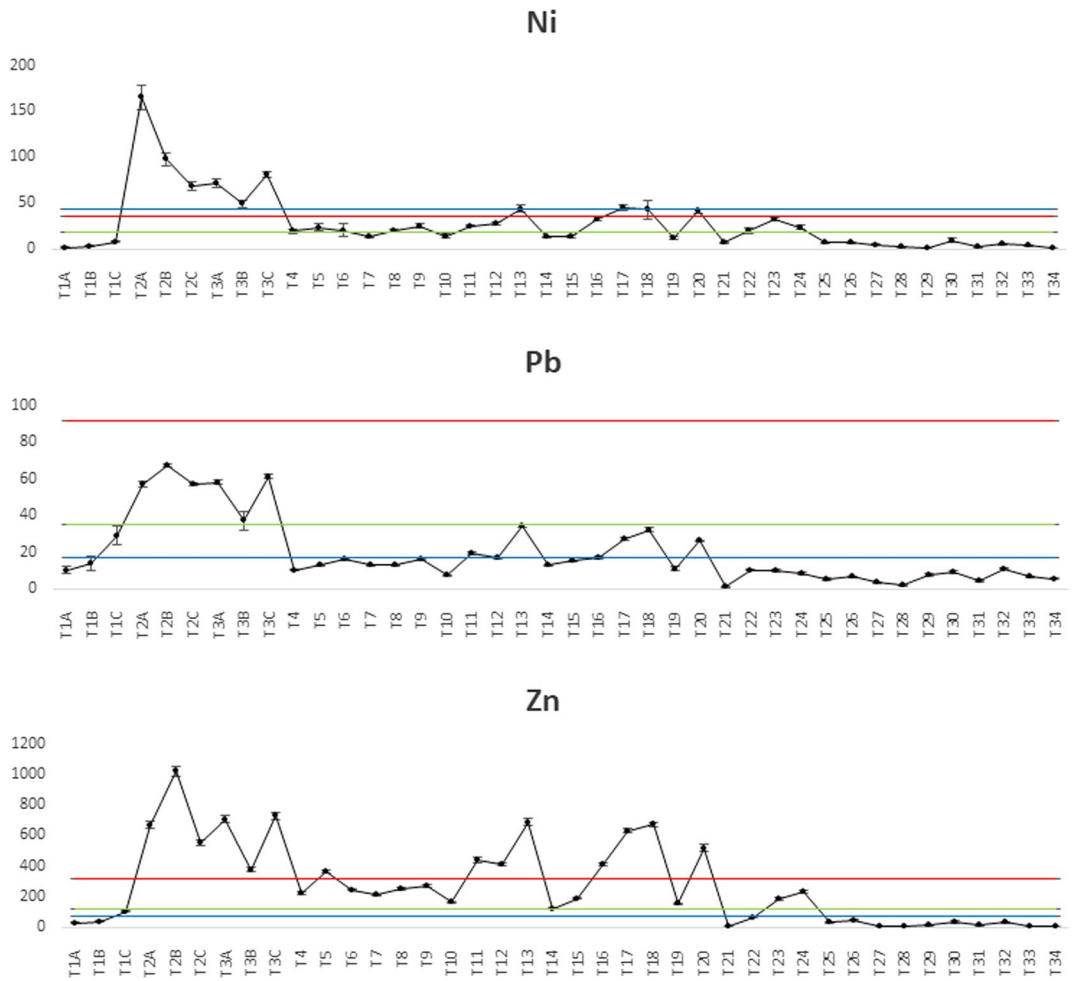

Fig. 3 (continued)

that these elements presented already baseline values well above the world average values.

Radionuclide's concentration in the sediments

The distribution of the activity concentration of the radionuclides in the sediment samples along the High, Middle and Low Tietê River and the corresponding Box Plots are presented in Figs. 6 and 7, respectively. Except for ^{210}Pb, all the radionuclides studied (^{238}U, ^{226}Ra, ^{232}Th, ^{228}Ra and ^{40}K) presented the same distribution, with activity concentrations decreasing from HTR to LTR region. In the LTR region the results are below the world average values available from UNSCEAR report [21] for ^{238}U, ^{226}Ra and ^{232}Th (no values for ^{228}Ra and ^{210}Pb are available in the UNSCEAR report).

The Box Plots for ^{238}U and ^{226}Ra in each region indicate that these radionuclides of the same radioactive decay series are in equilibrium in the sediments. The same behavior is observed for the radionuclides ^{232}Th and ^{228}Ra confirming the radioactive equilibrium in the Th decay chain. The radionuclide ^{210}Pb presented a value higher than its parent (^{226}Ra), indicating a possible anthropogenic contribution from the decay of ^{222}Rn gas present in the air and deposition in the sediments of the daughters of long half-life.

The median values obtained for the radionuclides ^{238}U, ^{226}Ra, ^{210}Pb, ^{232}Th, ^{228}Ra and ^{40}K in the box plots showed that their concentration decreases from HTR to LTR and that their distribution is representative of the lithology of each region, indicating different deposition and geochemical environments. No evidence was found of possible contamination by these radionuclides.

The distribution of the artificial radionuclide ^{137}Cs was not presented in Fig. 4, since its activity concentration was below the detection limit of the gamma spectrometer (<0.21 Bq kg^{-1}) in 80% of the results. The range observed for this element varied from 0.22 ± 0.08 Bq kg^{-1} to 0.96 ± 0.12 Bq kg^{-1}, that represent the base line of this radionuclide in the Tietê River sediments. The samples with

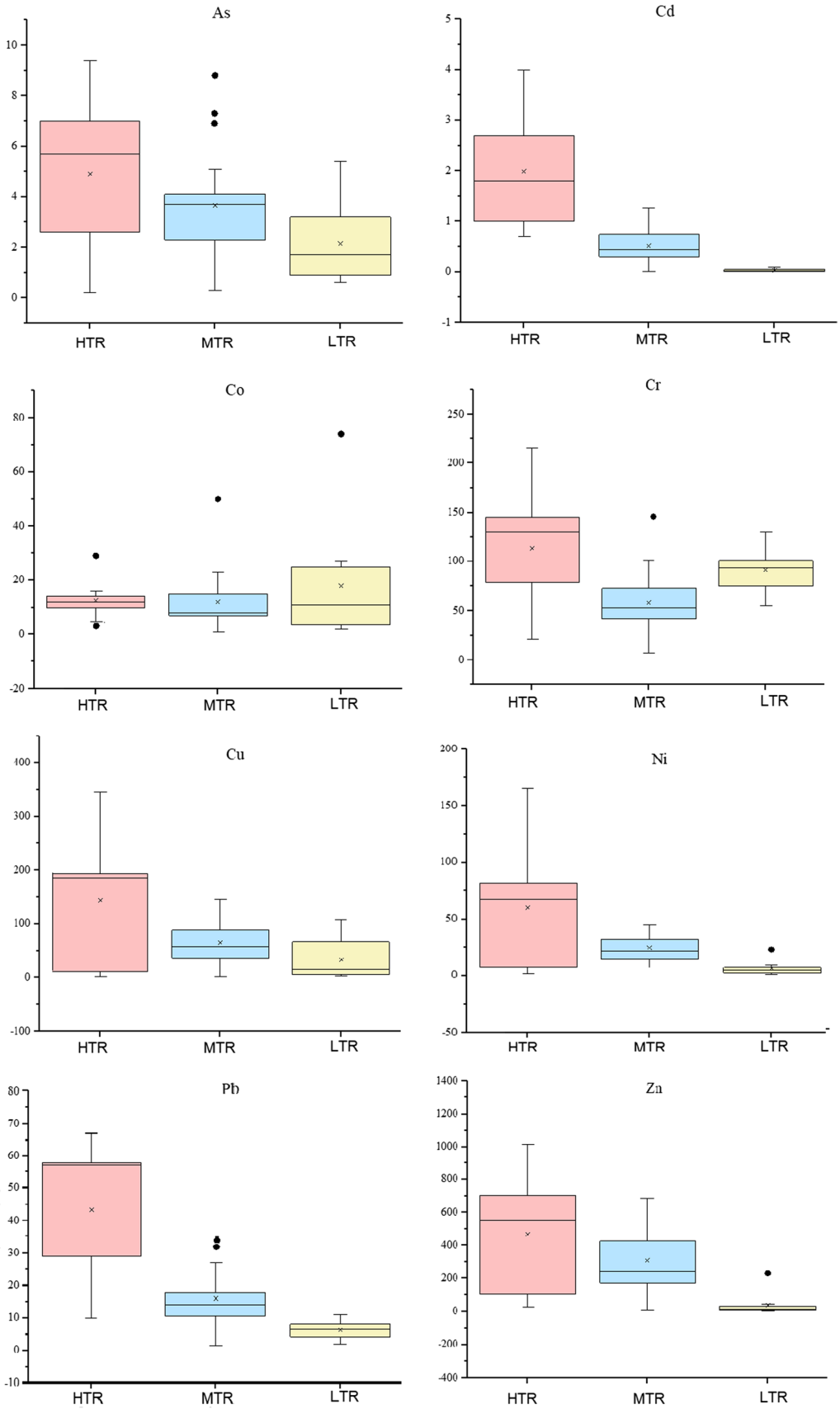

Fig. 4 Box Plot of the element's mass fraction (mg kg^{-1}) according to the region: HTR (T1 to T3), MTR (T4 to T23) and LTR (T24 to T34)

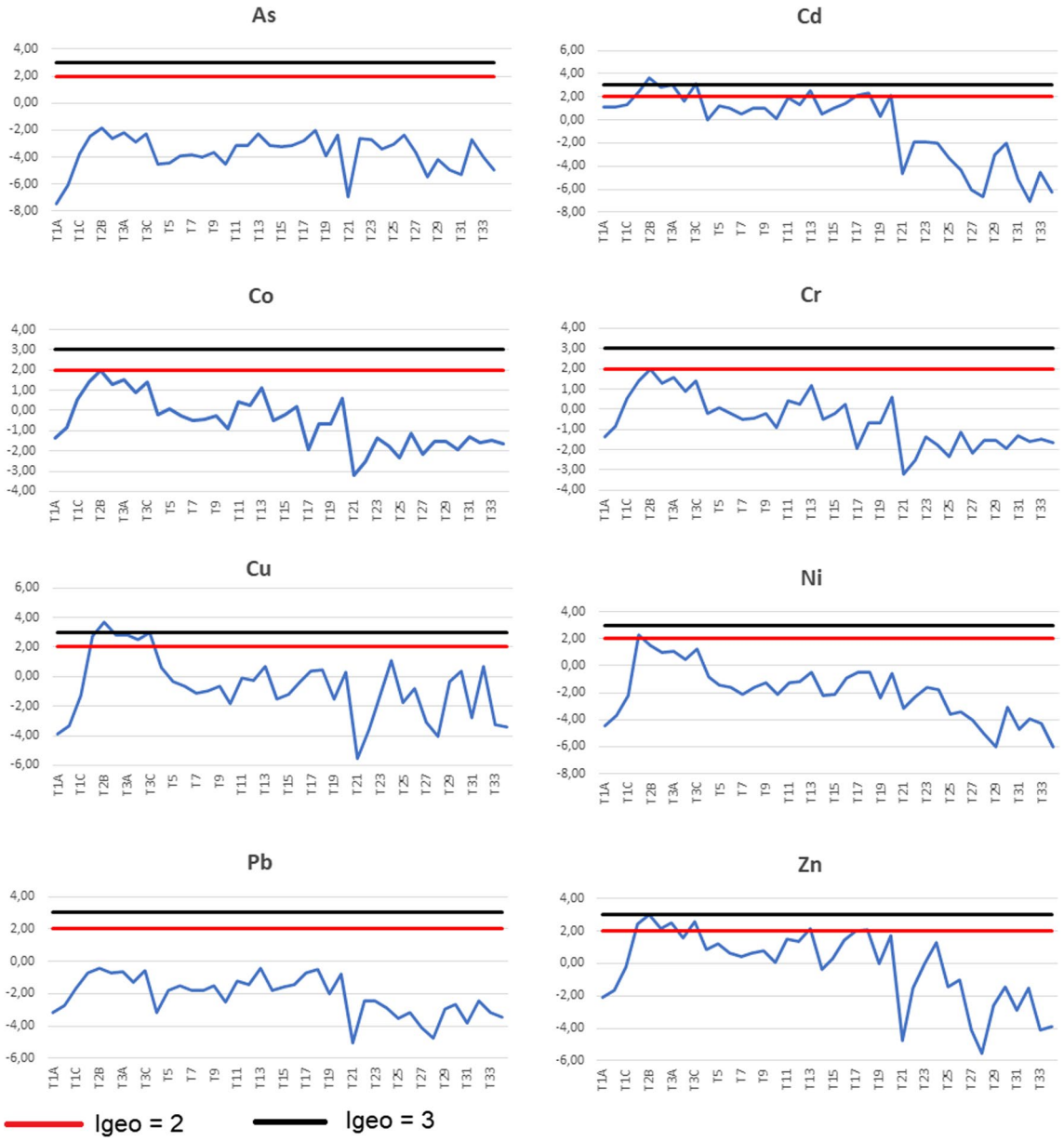

Fig. 5 *IGeo* values for the elements As, Cd, Co, Cr, Cu, Ni, Pb and Zn

measurable amounts of ^{137}Cs presented also high content of clay, giving evidence that this radionuclide tends to be absorbed by clays.

The sediments with higher concentration, outliers T1C, T6 and T26 for ^{232}Th; T26 for both ^{228}Ra and ^{238}U; T1C, T13, T17 and T18 for ^{226}Ra are predominantly made of silt and clay. On the other hand, the sediments with lower concentration, outliers T2A and T21 for ^{226}Ra and ^{228}Ra; T1C, T21 and T22 for ^{40}K; are predominantly made of sand.

The Cluster analysis was applied to identify groups of data that behave similarly, considering the major and trace elements mass fraction, radionuclides activity concentration and the sediment's grain size. The dendrogram is depicted in Fig. 8. It is observed that all the trace elements studied (As, Cd, Cr, Cu, Ni, Pb, ^{210}Pb and Zn) correlate well with the major elements Al_2O_3 and P_2O_5, and silt and clay. The natural radionuclides (^{238}U, ^{226}Ra, ^{232}Th, ^{228}Ra and ^{40}K) formed a distinct group with K_2O and Na_2O. Cobalt, which is from geogenic origin presented a strong correlation with the major components TiO_2, Fe_2O_3, CaO, MnO and MgO.

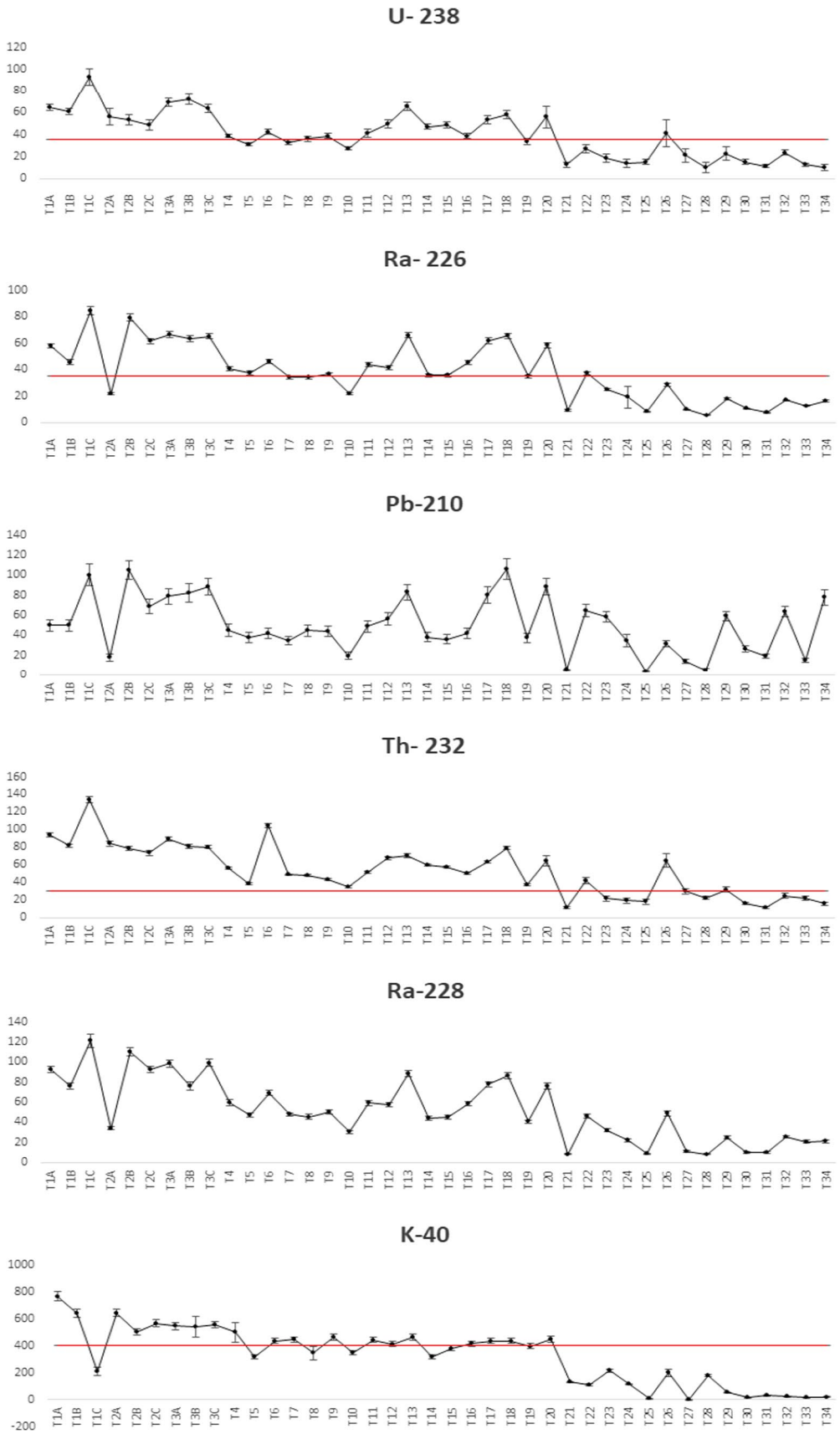

Fig. 6 Radionuclide's activity concentration in the sediments (Bq kg^{-1}) and UNSCEAR values (red line). Error bars represent expanded uncertainties at $k=2$

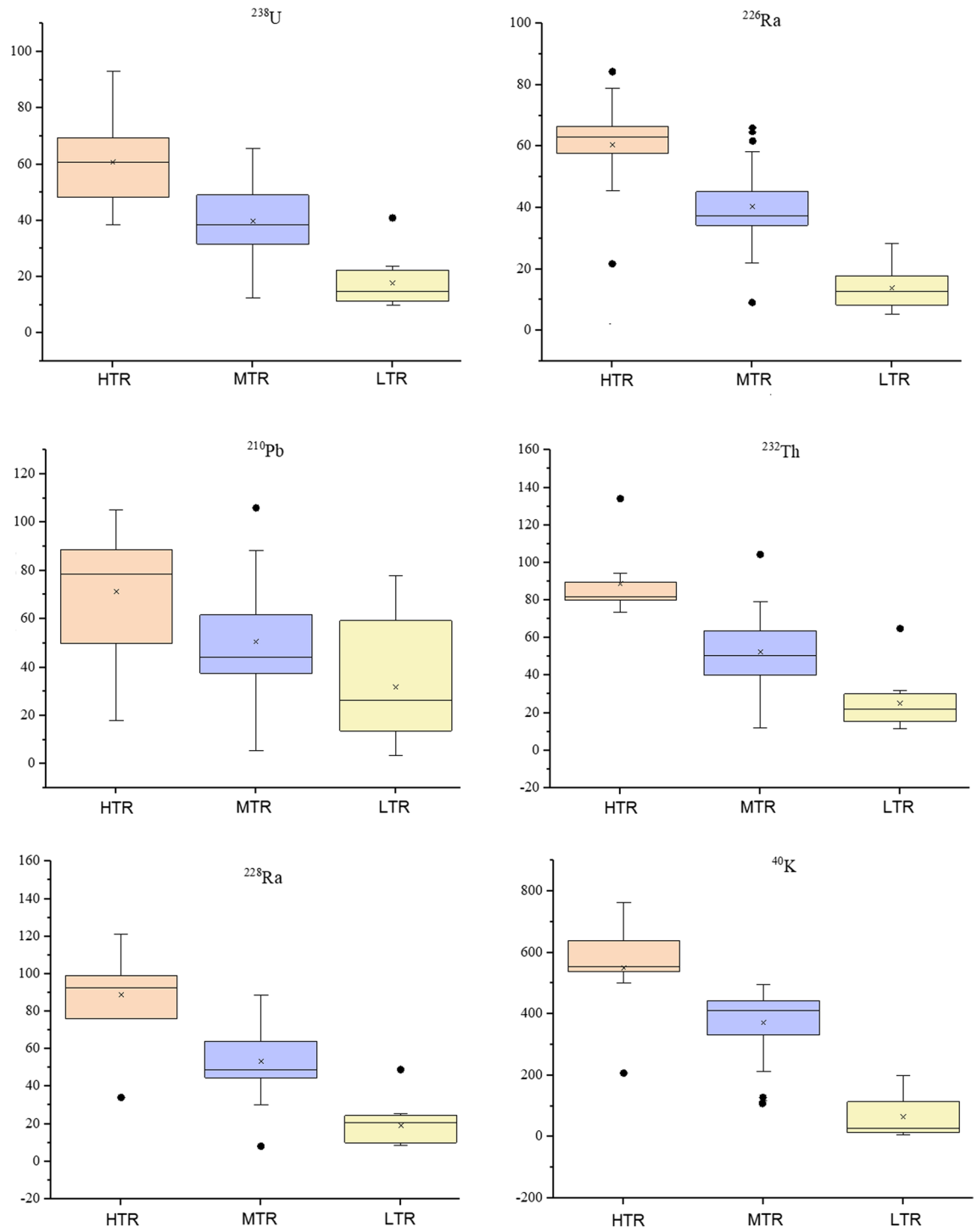

Fig. 7 Box Plot of the activity concentration of ^{238}U, ^{226}Ra, ^{210}Pb, ^{232}Th, ^{228}Ra and ^{40}K (Bq kg^{-1}) according to the region: HTR (T1 to T3), MTR (T4 to T23) and LTR (T24 to T34)

Conclusion

This study allowed to evaluate the basal levels of potentially contaminating elements (As, Cd, Co, Cr, Cu, Ni, Pb and Zn) and natural radionuclides, and to point out spots with high contamination that need special attention and mitigating measures.

The geoaccumulation index and the PEL values were used to assess whether the origin of the analyzed elements came from anthropogenic or natural sources. The *IGeo*

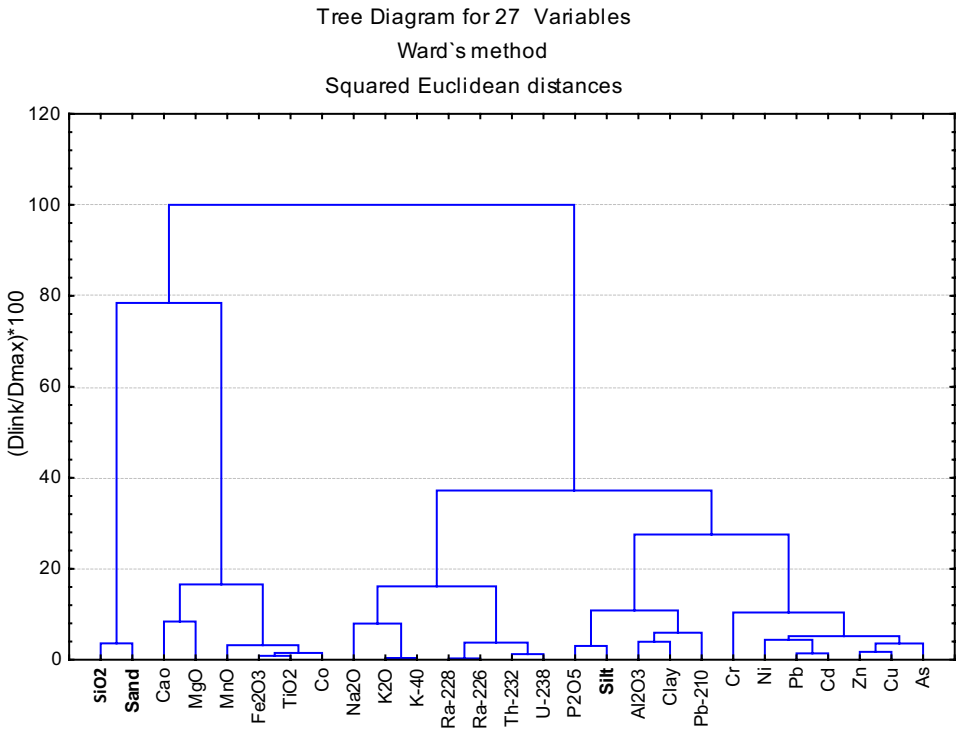

Fig. 8 Dendrogram of data considering the major and trace elements mass fraction, radionuclides activity concentration and the sediment's grain size

results obtained for Cd, Cr, Cu, Ni and Zn, using as reference local values of the region, indicated that the High Tietê region presents a high degree of contamination, followed by the Middle Tietê region; whereas the Low Tietê region did not present contamination. These results may confirm the anthropogenic influence of São Paulo Metropolitan Region, mainly related to untreated domestic sewage, industrial and agricultural effluents in the HTR. The results for the elements As and Pb showed that there was an improvement in the quality of the sediments, over the last 12 years, although these elements presented basal values well above the world average values.

The Tietê River tributaries play an important role in the pollution observed in this river, since they transport considerable amounts of pollutants, into the river.

The concentration levels of natural radionuclides (^{238}U, ^{226}Ra, ^{210}Pb, ^{232}Th, ^{228}Ra and ^{40}K) and ^{137}Cs in sediment samples along the Tietê River were determined for the first time, which is a contribution of the present study. The natural radionuclide concentrations were of the same order of magnitude of world average values and can be defined as basal levels of the region. The results of ^{137}Cs, ranging from 0.22 ± 0.08 Bq kg^{-1} to 0.96 ± 0.12 Bq kg^{-1}, represent the base line of this radionuclide in the Tietê River sediments.

Acknowledgements This project was supported by Fundação de Amparo à Pesquisa do Estado de São Paulo (FAPESP), research contract 2014/20805-6, and by Conselho Nacional de Desenvolvimento Científico e Tecnológico (CNPq), grants 300835/95-7 and 308660/2019-6.

References

1. Mortatti J, Hissler C, Probst JL (2010) Heavy metal distribution in the bottom sediments along Tietê River basin. Revista do Instituto de Geociências, Geologia 10(2):3–11
2. Campos APS (2012) A presença de metais e compostos químicos orgânicos nas águas superficiais e nos sedimentos do rio Tietê. Tese (Doutorado em Saúde Pública) Faculdade de Saúde Pública da Universidade de São Paulo, São Paulo
3. Rocha FR, Silva PSC, Castro LM, Bordon ICCL, Oliveira SMB, Favaro DIT (2015) NAA and XRF technique bottom sediment assessment for major and trace elements: Tietê River, São Paulo State. Brazil J Radioanal Nucl Chem 306(3):655–665
4. Favaro DIT, Rocha FR, Angelini M, Henriques HRA, Soares JS, Silva PSC, Oliveira SMB (2018) Metal, major and trace element assessment of Tietê River sediments from medium Tietê River basin, Sao Paulo State, Brazil: part II. J Radioanal Nucl Chem 316(2):805–818
5. Larrizzatti FE, Favaro DIT, Moreira SRD, Mazzilli BP, Piovano EL (2001) Multielemental determination by instrumental neutron activation analysis and recent sedimentation rates using ^{210}Pb dating method at Laguna del Plata, Cordoba. Argentina J Radioanal Nucl Chem 249(1):263–268
6. Konieczka P, Namiesnik J (2009) Quality assurance and quality control in the analytical chemical laboratory: a practical approach. CRC Press, Florida. https://doi.org/10.1201/9781420082715
7. USEPA (2007) Method 3051A.Microwave assisted acid digestion of aqueous samples and extracts. http://www.epa.gov/sites/production/files/2015–12/documents/3015a.pdf. Accessed in Set 2020

8. INMETRO—Instituto Nacional de Metrologia, Qualidade e Tecnologia. Orientação sobre Validação de Métodos Analíticos. Coordenação Geral de Acreditação, DOQ-CGCRE-008, revisão 3. 2010
9. Tappiz B, Moreira EG (2021) Expanded uncertainty assessment in fish samples analyzed by INAA and AAS. Braz J Radiat Sci 9(1A):1–14
10. Mori PE, Reeves S, Correia CT, Haukka M (1999) Development of a fused glass disc XRF facility with pressed powder pellet technique at Instituto de Geociencias. São Paulo Univ Rev Bras Geoc 29(3):441–446
11. Govindaraju K (1989) Compilation of working values and sample description of 272 geostandards. Geostandard Newsletter 13:1–113
12. Cutshall N, Larsen IL, Olsen CR (1983) Direct analysis of ^{210}Pb in sediment samples: absorption corrections. Nuclear Instruments Methods 206:309–312
13. Camargo AO, Moniz AC, Jorge JA, Valadares JMAS (2009) Métodos de análise química e física de solos do IAC. Boletim Técnico, 106, Campinas, IAC
14. IPT—Instituto de Pesquisas Tecnológicas (1981) Mapa Geológico do Estado de São Paulo, São Paulo, Brasil, V1 (IPT-Monografias)
15. Taylor SR, McLennan SM (1985) The continental crust: its composition and evolution. Blackwell Scientific, London
16. CCME (1995) Canadian council of ministers of the environment. Protocol for the derivation of Canadian Sediment quality guidelines for the protection of aquatic life.
17. Silva PSC, Damatto SR, Maldonado C, Favaro DIT, Mazzilli BP (2011) Metal distribution in sediment cores from Sao Paulo State Coast, Brazil. Mar Poll Bull 62:1130–1139
18. Gomes FC, Godoy JM, Godoy MLDP, Carvalho ZL, Lopes RT, Sanchez-Cabeza JA, Lacerda LD, Wasserman JC (2009) Metal concentrations, fluxes, inventories and chronologies in sediments from Sepetiba and Ribeira Bays: a comparative study. Mar Poll Bull 59:123–133
19. Rezaee KH, Abdi DIMR, Saion EB (2011) Distribution of trace elements in the marine sediments along the South China Sea. Malaysia J Radioanal Nucl Chem 287(3):733–740
20. Nascimento MRL, Mozeto AA (2008) Reference values for metals and metalloids concentrations in bottom sediments of Tietê River Basin, Southeast of Brazil. Soil Sedim Contam 17:269–278
21. UNSCEAR (2000) Sources and effects of ionizing radiation, United Nations Scientific Committee on the Effects of Atomic Radiation UNSCEAR 2000 Report to the General Assembly, with Scientific Annexes